Treating Late-Time Instability of Hybrid Finite-Element/Finite-Difference Time-Domain Method

Chieh-Tsao Hwang and Ruey-Beei Wu

***Abstract*— The hybrid finite-element/finite-difference time-domain (FETD/FDTD) method recently proposed to handle arbitrarily shaped dielectric objects is employed to investigate electromagnetic problems of high Q systems for which the transient response over a very long duration is necessary. To begin with, the paper demonstrates that this hybrid method may suffer from late-time instability and spurious dc modes. Then an approach which combines the temporal filtering and frequency shifting techniques is presented to overcome sequentially and, respectively, the two drawbacks. Its accuracy is validated by the favorable comparison with several different methods for the analysis of resonant frequencies and Q factors of the various modes in an isolated dielectric resonator. Finally, the present method is applied to calculate the scattering parameters on the microstrip line due to the presence of the cylindrical dielectric resonator.**

***Index Terms*— FDTD methods, finite-element methods, instability.**

I. Introduction

THE finite-difference time-domain (FDTD) method has been widely used in various electromagnetic problems [1]. In its original form, the method works excellently for structures, which can fit well into Cartesian coordinates [2]. The algorithm provides a lot of attractive advantages: direct and explicit time marching, high accuracy with discretization error of second order, obvious stability condition, easy programming, and minimum computational complexity. One of the major disadvantages of FDTD is the inefficiency to model the structures with curved surfaces.

Exploiting conformity is one way to alleviate the staircasing approximation [3]–[5]. Recently, a hybrid method has been proposed to solve the electromagnetic scattering of two- (2-D) or three-dimensional (3-D) arbitrarily shaped dielectric objects [6], [7]. It successfully employs the conventional FDTD method for most of the regular region but introduces the tetrahedral edge-based finite-element time-domain (FETD) scheme to model the region near the curved surfaces. Numerical results of early-time simulation validate that the method has the advantages of accuracy, flexibility, stability, and computational efficiency.

Manuscript received July 9, 1997; revised August 21, 1998. This work was supported in part by the National Science Council, Republic of China, under Grant NSC 88-2213-E-002-057.

The authors are with the Department of Electrical Engineering, National Taiwan University, Taipei, Taiwan, 10617 R.O.C.

Publisher Item Identifier S 0018-926X(99)03736-9.

However, instability happens in late-time simulation for FDTD methods with unstructured nonorthogonal grids or more general conformal models. This instabilities were noticed during the integral equation based time marching [8], [9] and several attempts have also been suggested to overcome it [10]–[12]. For the time marching based on the differential equations, like FDTD or finite-element method (FEM), late-time instability did not receive much attention until recently. Yee *et al.* noticed that the computational error grows up in the additional local coordinate system near the curved surfaces and suggested a spatial average scheme to resolve this instability [5]. On the other hand, some researchers applied the concept of time average to suppress the instability [13]–[15]. This paper is focused on treating the late-time instability of the hybrid FETD/FDTD method proposed in [6] and [7].

The late-time simulation is essential to investigate the electromagnetic characteristics of high Q systems. A salient example of common interest is the cylindrical dielectric resonator (DR). Several approaches have been presented to deal with an isolated DR such as the method of lines [16], the method of moments based on the surface integral equation [17], the null-field method [18], and FDTD in cylindrical coordinate [19]. However, to our knowledge, none of them have been generalized to deal with practical problems where the DR is coupled to the nearby guiding structures such as microstrip lines.

Following this introductory section, the hybrid FETD/FDTD method for arbitrarily shaped dielectric objects is briefly mentioned in Section II. The late-time instability is demonstrated and temporal filtering technique is proposed to suppress the instability. Then, an annoying phenomenon of linearly growing curl-free fields is noticed and explained in Section III. A novel frequency shifting technique which introduces an artificial term into the governing wave equation is proposed to circumvent these spurious modes. In Section IV, the present method is applied to investigate the electromagnetic characteristics of an isolated DR and a DR loaded with a microstrip line. Finally, brief conclusions are drawn in Section V.

II. Temporal Filtering Technique for Late-Time Instability

Even for the problems of dielectric objects with complicated shape, most of the solution region is homogeneous and can be handled by FDTD with rectangular grids. Only for the region close to the curved boundary, the general tetrahedral mesh

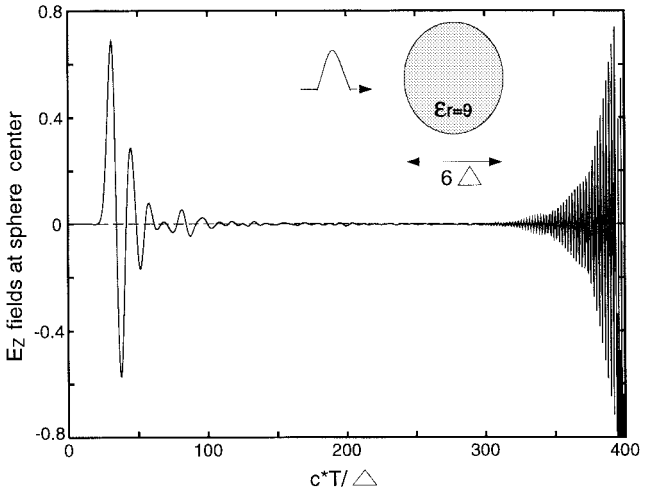

Fig. 1. The total E_z field versus the normalized time at the center of a dielectric sphere, which is of dielectric constant $\epsilon_r = 9$, radius three unit, and illuminated by an incident $\hat{z}$-polarized Gaussian plane wave of 3σ half-width $c \cdot T = 10\triangle$.

should be resorted to for an accurate modeling [6], [7]. In this irregular region, the electric field satisfies the governing equation

$$\nabla \times \nabla \times \vec{E} + \mu\epsilon \frac{\partial^2 \vec{E}}{\partial t^2} = 0. \tag{1}$$

By employing the time-domain finite-element method (FEM), this equation can be discretized into a matrix form of

$$\left([C] + \frac{\Delta_t^2}{4}[D]\right)\overline{E}^{n+1} = 2\left([C] - \frac{\Delta_t^2}{4}[D]\right)\overline{E}^{n} - \left([C] + \frac{\Delta_t^2}{4}[D]\right)\overline{E}^{n-1} \tag{2}$$

where

$$[C]_{ij} = \int_\Omega \epsilon \vec{W}_i \cdot \vec{W}_j \, d\Omega$$
$$[D]_{ij} = \int_\Omega \frac{1}{\mu} \nabla \times \vec{W}_i \cdot \nabla \times \vec{W}_j \, d\Omega.$$

$\triangle_t$ is the discretization in time, $\overline{E}$ denotes the coefficient vector for unknown fields with superscript standing for the time step, and $\vec{W}_i$ is the Whitney one-form edge element [20].

The hybrid FETD/FDTD has been employed to deal with the scattering of arbitrarily shaped dielectric cylinders [6] and 3-D objects [7]. It is worth mentioning that the hybrid method invokes FDTD for the outer region. As a result, the unsplit and modified perfectly matching layers (PML's) [21], [22] can be imposed to truncate the simulation region without any difficulty. For the sake of simplicity, we consider the 3-D scattering problem in [7], where a plane wave of Gaussian waveform is incident on a dielectric sphere. Fig. 1 shows the electric field versus the normalized time at the center of the sphere. It demonstrates that the computational error may accumulate to grow up when the simulation is performed up to a very late time.

The late-time instability cannot be contributed to the FETD scheme (2) since which has been theoretically shown to be unconditionally stable [23]. To investigate the source of the instability, A perfectly electrical conductor (PEC)-walled cubic cavity under a line current source excitation is simulated by applying the pure FDTD, pure FETD, and hybrid FETD/FDTD methods, respectively. Although not displayed here, late-time instability only occurred in the hybrid FETD/FDTD method. It is believed that the late-time instability is due to the interface between FEM and FDTD solutions. The strategy employed here is to derive a low-pass filter which can suppress the computational error which is of higher frequencies and in the meantime keeps the low-frequency components nearly unchanged. Here, the filter is defined by the relation [13]

$$F(n) = bf(n+1) + qf(n) + pF(n-1) \tag{3}$$

where F and f denote the filtered and original fields, respectively, and b, q, and p are unknown constants to be specified.

To have a zero attenuation at dc frequency, the constants should satisfy

$$b + q + p = 1. \tag{4}$$

In addition, we choose

$$b = p \tag{5}$$

to make (3) a symmetric form. From (4) and (5), the constant q can be related to p by

$$q = 1 - 2p. \tag{6}$$

The remaining constant p can be chosen arbitrarily. The parameter p should be large enough to suppress the instability. However, the larger the value p is, the stronger attenuation and phase delay (3) will effect the time-domain response. We ran a number of test cases to observe the effect on stability with p as a parameter. All cases were run over 20 000 time iterations and it is found that the late-time instability did not occur as the value of p equals or exceeds 0.05.

To verify the performance of this filter, the relation (3) with $p = 0.05$ is applied to modify the electric fields at time step n in entire FEM region after obtaining the fields at time step $n+1$ from the FEM solver. Fig. 2 shows the simulation results modified by the temporal filtering technique for the 3-D scattering problem considered in Fig. 1. In the early-time response shown in Fig. 2(a), the desired signal is hardly affected by the enforcement of this filter. In the late-time response shown in Fig. 2(b), it is verified that the instability due to the computational errors has been successfully suppressed.

III. Frequency Shifting Technique for Spurious Curl-Free Mode

A magnified view of the filtered late-time response in Fig. 2(b) reveals that there are spurious components which grow linearly with time. The occurrence is replotted as the solid curve in Fig. 3 where the vertical axis is in a different scale from Fig. 2(b). This spurious mode can be attributed to the insufficiency of (1) to model the Maxwell's equations at the dc limit. It is not difficult to show that (1) has a nontrivial solution of the form

$$\overline{E}_s = -\nabla \phi \cdot t \tag{7}$$

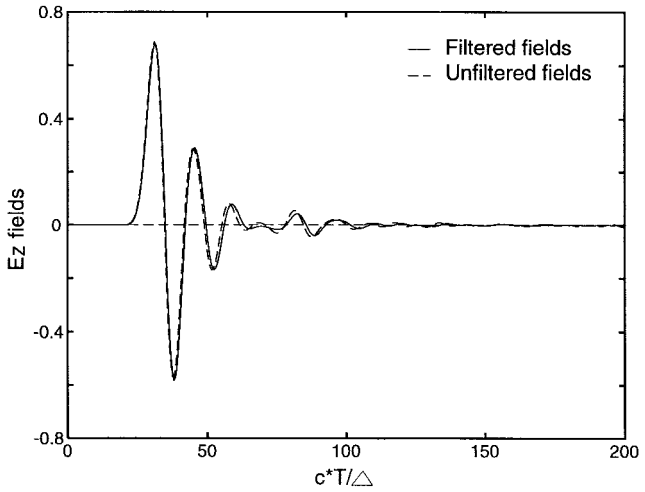

Fig. 2. Comparisons between filtered and original fields shown in Fig. 1. (a) Early-time response. (b) Late-time response.

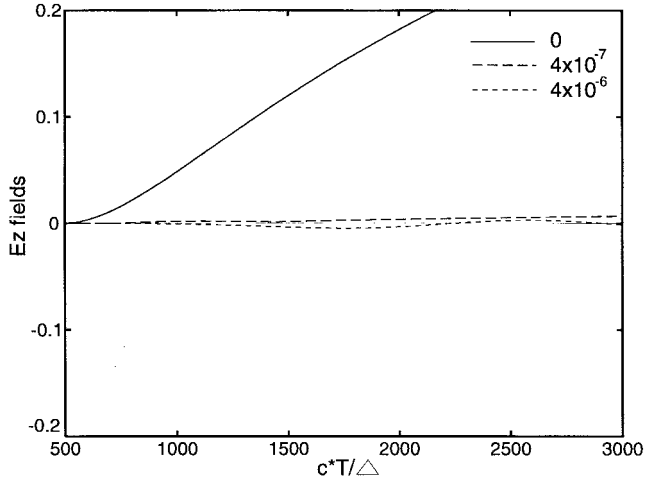

Fig. 3. Effects of the frequency shifting on the filtered response shown in Fig. 2. The shift value δ is chosen as zero (no shift), $4 \times 10^{-7}(\mu\epsilon/\triangle_t^2)$ and $4 \times 10^{-6}(\mu\epsilon/\triangle_t^2)$.

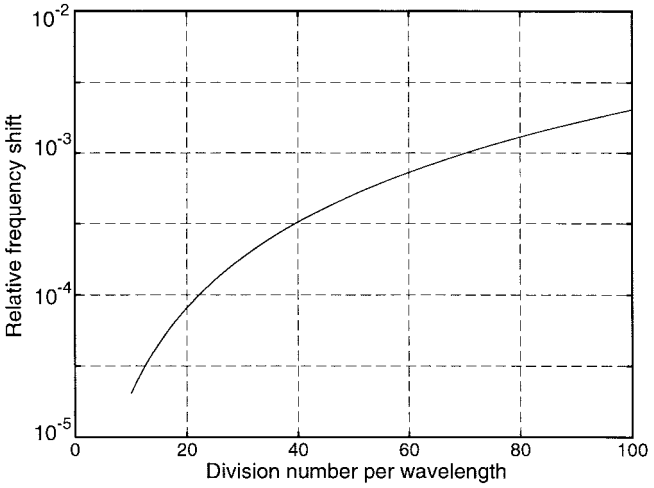

Fig. 4. Relative frequency shift $(\omega - \omega_0/\omega_0)$ versus division number per wavelength for the case $\delta = 4 \times 10^{-6}(\mu\epsilon/\triangle_t^2)$.

for arbitrary scalar function $\phi(\vec{r})$. This field distribution is curl-free in space but grows linearly with respect to time. It means that any curl-free distribution once generated, no matter how small, will grow up to be the most dominating in the very late time. Actually, this phenomenon happens to some other time marching schemes which relies solely on the electric field wave equation (1), e.g., [12]. For the present method, it is the FETD/FDTD boundary that excites this irrational field. For the FDTD simulation, which takes curl operation for the electric field in the previous time step to update the magnetic field in the present time step, this spurious mode will be suppressed and have no chance to grow up.

A good way to destroy the linear growth of the spurious modes is to change the nontrivial solution (7) by slightly modifying the governing equation (1) into

$$(\bigtriangledown \times \bigtriangledown \times + \delta)\vec{E} + \mu\epsilon \frac{\partial^2 \vec{E}}{\partial t^2} = 0 \tag{8}$$

where δ is a small positive constant. Then, the nontrivial solution (7) becomes

$$\overline{E}_s = - \bigtriangledown \phi \cdot \cos(\omega_\delta t) \tag{9}$$

with an angular frequency of $\omega_\delta \equiv \sqrt{\delta/\mu\epsilon}$. It is worthy mentioning that this field pattern remains a small variation, rather than growing up linearly with respect to time. Also note that the numerical solution for (8) is almost the same as that for (1), except that the matrix $[D]$ in (2) is replaced by $[D] + \omega_\delta^2[C]$. In addition to suppressing the spurious modes, the constant δ in (8) also introduces frequency shifts for all the signal components. Consider the plane wave component of the form $e^{j(\omega t - \vec{k}\cdot\vec{r})}$. The dispersion relation given by (8) is

$$\omega^2 = \omega_0^2 + \omega_\delta^2 \tag{10}$$

where $\omega_0 = k/\sqrt{\mu\epsilon}$ denotes the corresponding angular frequency in the original equation (1).

The best choice of δ will be the smallest one which is able to suppress the linear growth of the spurious modes. Numerical experiments have been evoked to find this δ. Fig. 3 shows the simulation results with $\delta = 4 \times 10^{-6}(\mu\epsilon/\triangle_t^2)$ and $4 \times 10^{-7}(\mu\epsilon/\triangle_t^2)$ as a parameter. After extensive trial, it is found that $\delta = 4 \times 10^{-6}(\mu\epsilon/\triangle_t^2)$ is enough to destroy the linear growth of spurious modes. Fig. 4 shows the resultant

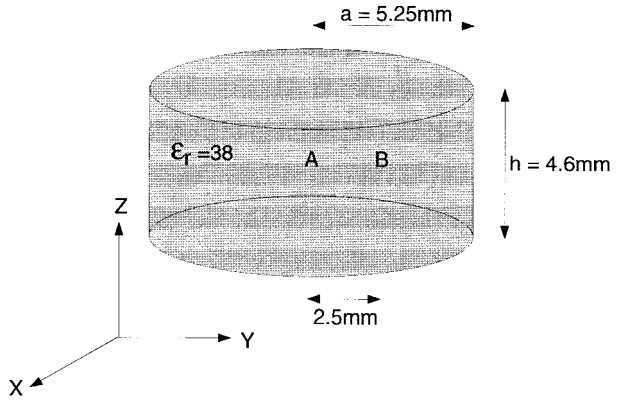

Fig. 5. Geometry of a dielectric resonator.

TABLE I
(a) COMPARISON OF THE CALCULATED RESONANT FREQUENCIES OF VARIOUS RESONANT MODES IN DR, SHOWN IN FIG. 5 BY SEVERAL DIFFERENT METHODS. (b) COMPARISON OF THE CALCULATED Q FACTORS OF VARIOUS RESONANT MODES IN DR, SHOWN IN FIG. 5 BY SEVERAL DIFFERENT METHODS

Method	k_0a of resonant modes			
	$TE_{01\delta}$	$HEM_{11\delta}$	$HEM_{12\delta}$	$TM_{01\delta}$
MoL [13]	0.537	0.696	0.732	0.827
MoM [14]	0.531	0.696	0.730	0.827
Null-field [15]	0.534	0.698	0.731	0.829
2D FDTD [16]	0.535	0.698	0.731	0.827
Measurement [21]	0.533	0.696	0.726	0.824
Staircased FDTD($a = 10\triangle$)	0.539	0.704	0.739	0.792
Staircased FDTD($a = 21\triangle$)	0.536	0.694	0.732	0.825
Present method($a = 10\triangle$)	0.531	0.691	0.726	0.817
Present method($a = 21\triangle$)	0.534	0.698	0.728	0.823

(a)

Method	Q-factor of resonant modes			
	$TE_{01\delta}$	$HEM_{11\delta}$	$HEM_{12\delta}$	$TM_{01\delta}$
MoL [13]	43.73	31.46	48.55	72.96
MoM [14]	45.8	30.7	52.1	76.8
Null-field [15]	40.80	30.85	50.30	76.90
2D-FDTD [16]	47	31	46	71
Measurement [21]	46.4	30.3	43.3	58.1
Staircased FDTD($a = 10\triangle$)	33.49	17.93	34.82	35.03
Staircased FDTD($a = 21\triangle$)	35.68	28.21	42.37	74.56
Present method($a = 10\triangle$)	38.01	28.48	46.48	72.90
Present method($a = 21\triangle$)	36.81	28.81	49.42	77.72

(b)

relative frequency shift $(\omega - \omega_0)/\omega_0$ versus division number per wavelength. In the frequency range of common interest that the wavelength λ is 10–100 times the division size, the relative frequency shift varies from 2×10^{-5} to 2×10^{-3}.

IV. NUMERICAL RESULTS

A. Isolated Dielectric Resonator

The late-time simulation is essential for the analysis of the structures in which high Q elements are involved. In this paper, the hybrid FETD/FDTD together with the aforementioned stabilizing approach is applied to deal with the dielectric resonators (DR). The first example considers an isolated DR, which has been tacked by various methods [16]–[19]. The DR is made of the dielectric with $\epsilon_r = 38$ and has the geometry

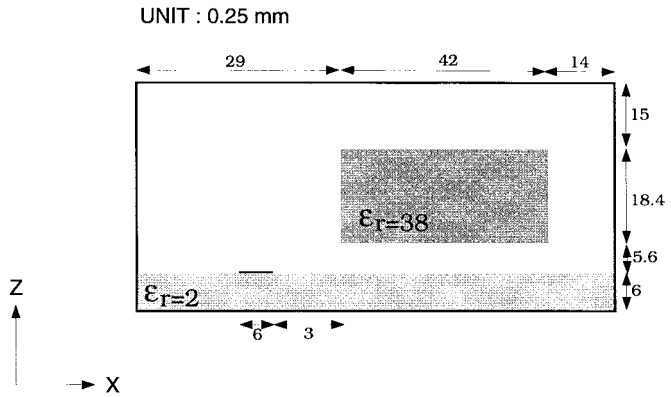

(a)

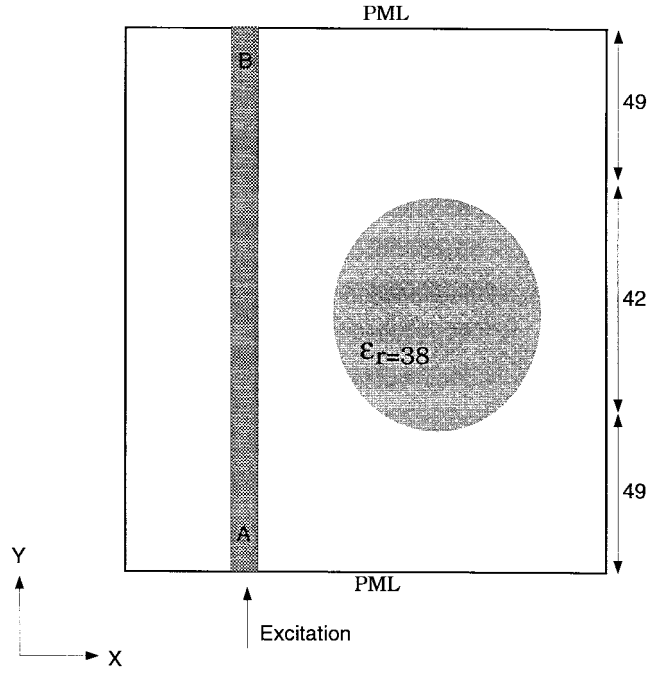

(b)

Fig. 6. A typical structure where a dielectric resonator is mounted with a microstrip line. A modulated Gaussian pulse is incident to the microstrip line.

parameters of radius $a = 5.25$ mm and height $h = 4.6$ mm, as shown in Fig. 5.

In the simulation, the FDTD cell is chosen to be $\triangle = a/21$ and the time step $\triangle_t$ is such that the stability factor $\rho = (c \cdot \triangle_t)/\triangle = 0.5$. Among which, the outermost eight layers are placed unsplit and modified PML [21], [22]. The excitation source is chosen to have the modulated Gaussian waveform with sinusoidal time variant function. The source is either a uniform $\hat{z}$-directed electrical or magnetic line current source spanning a length of 3.75 mm at the center of DR, i.e., point A in Fig. 5. For the present case, 147 611 tetrahedral cells and 190 648 edges are used to model the region near the dielectric resonator boundary.

The recorded signals can be represented by the summation of several damped sinusoidal functions, each of which denotes a mode. The number of significant modes and the modal parameters, i.e., the resonant frequency and the Q factors, can be extracted from the recorded responses by the matrix pencil

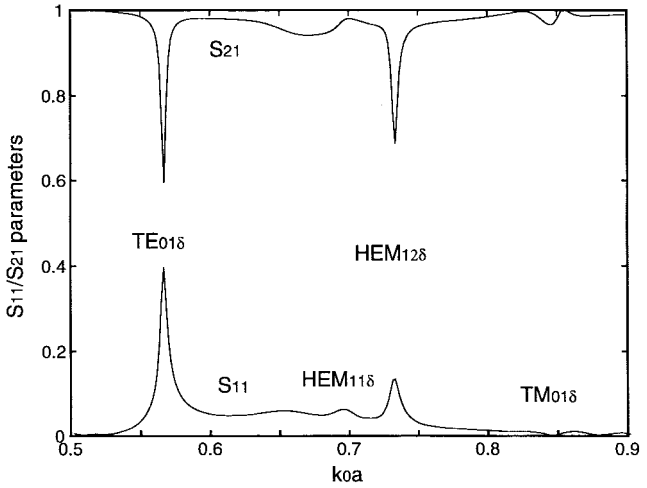

Fig. 7. Reflected and transmitted coefficients versus normalized wave number ($k_0 a$).

technique [24]. The results are listed in Table I and compared with those by other methods, e.g., the method of line [16], the method of moments [17], the null-field method [18], 2-D FDTD in angularly symmetric structures [19], pure FDTD with staircase approximation, as well as the measurement results [25]. The good agreement validates the correctness of the present method. In Table I, the FDTD simulations with a rough division of $\triangle = a/10$ are also included for comparison. It can be verified that the present method with a rough division can still yield accurate results, especially for Q factors, while the staircasing FDTD can not.

B. Dielectric Resonator Mounted with Microstrip Line

In practical microwave circuits, DR's are placed in the nearby of microstrip lines to serve as frequency selecting elements as shown in Fig. 6. In the simulation, the same DR considered in Fig. 5 is mounted with a microstrip line of substrate dielectric constant $\epsilon_r = 2$. The structure is enclosed by the metallic walls except the input and output sides of the microstrip lines, where the PML are placed to absorb the scattered fields. An excitation source with modulated Gaussian waveform is incident to one end of the microstrip line.

To achieve a high resolution in the frequency domain, the waveforms should extend to an extraordinarily long period. Fortunately, the late-time responses can be expressed almost solely by the DR modes, which are extracted by applying the matrix pencil technique from the waveform up to $4200\triangle_t$. These contributions of the DR modes are then extrapolated to give the responses over an extended duration of $2^{17} \cdot \triangle_t$ in time.

Fig. 7 shows the resultant scattering parameters versus frequency obtained from the responses of extended duration by inverse FFT. Please notice the very sharp variations near the resonant frequencies of the DR modes. Among the modes recognized in Table I(a), the $\mathrm{TE}_{01\delta}$ mode exhibits strongest coupling with the microstrip line. The hybrid modes $\mathrm{HEM}_{11\delta}$ and $\mathrm{HEM}_{12\delta}$ also appear noticeable effects. However, the $\mathrm{TM}_{01\delta}$ mode of DR seems to be orthogonal with the guided microstrip line mode and, consequently, no reflected field is observed at its resonant frequency.

V. Conclusions

In this paper, we have presented two techniques to eliminate late-time instabilities and spurious modes arising in the hybrid time marching scheme, which combines rectangular-grid FDTD with tetrahedral-grid FEM. The procedure involves applying a low-pass filter in time to stabilize high-frequency computational noise and introducing slight frequency shift into the governing wave equation to eliminate the linear growth of spurious modes. The approach has been applied to deal with the dielectric resonators problems. Its capability to deal with the electromagnetic systems including high Q elements has been demonstrated and verified.

References

[1] A. Taflove, *Computational Electrodynamics: The Finite-Difference Time-Domain Method.* Norwood, MA: Artech House, 1995.
[2] K. S. Yee, "Numerical solution of initial boundary value problems in isotropic media," *IEEE Trans. Antennas Propagat.,* vol. AP-14, pp. 302–307, May 1966.
[3] R. Holland, "Finite-difference solutions of Maxwell's equations in generalized nonorthogonal coordinates," *IEEE Trans. Nuclear Sci.,* vol. NS-30, pp. 4589–4591, Dec. 1983.
[4] T. G. Jurgens, A. Talflove, K. Umashanker, and T. G. Moore, "Finite-difference time-domain modeling of curved surfaces," *IEEE Trans. Antennas Propagat.,* vol. 40, pp. 357–366, Apr. 1992.
[5] K. S. Yee, J. S. Chen, and A. H. Chang, "Conformal finite-difference time-domain (FD-TD) with overlapping grid," *IEEE Trans. Antennas Propagat.,* vol. 40, pp. 1068–1075, Sept. 1992.
[6] R. B. Wu and T. Itoh, "Hybridizing FD-TD analysis with unconditionally stable FEM for objects of curved boundary," in *IEEE MTT-S 1995 Int. Microwave Symp. Dig.,* Orlando, FL, May 1995, pp. 833–836.
[7] ——, "Hybrid finite-difference time-domain modeling of curved surfaces using tetrahedral edge elements," *IEEE Trans. Antennas Propagat.,* vol. 45, pp. 1302–1309, Aug. 1997.
[8] C. L. Bennett and H. Mieras, "Time domain scattering from open conducting surfaces," *Radio Sci.,* vol. 10, pp. 1231–1239, Nov./Dec. 1981.
[9] S. M. Rao and D. R. Wilton, "Transient scattering by conducting surfaces of arbitrary shape," *IEEE Trans. Antennas Propagat.,* vol. 39, pp. 56–61, Jan. 1991.
[10] A. G. Tijhuis, "Toward a stable marching-on-in-time method for two-dimensional electromagnetic scattering problems," *Radio Sci.,* vol. 19, pp. 1311–1317, Sept./Oct. 1984.
[11] A. Sadigh and E. Arvas, "Treating the instabilities in marching-on-in-time method from a different perspective," *IEEE Trans. Antennas Propagat.,* vol. 41, pp. 1695–1702, Dec. 1993.
[12] R. S. Adve, T. K. Sarkar, O. M. C. Pereiar-Filho, and S. M. Rao, "Extrapolation of time-domain responses from three-dimensional conducting objects utilizing the matrix pencil technique," *IEEE Trans. Antennas Propagat.,* vol. 45, pp. 147–156, Jan. 1997.
[13] D. J. Riley and C. D. Turner, "VOLMAX: A solid-model based, transient volumetric Maxwell solver using hybrid grids," *IEEE Antennas Propagat. Mag.,* vol. 39, pp. 20–33, Feb. 1997.
[14] S. Palaniswamy, W. F. Hall, and V. Shankar, "Numerical solution to Maxwell's equations in the time domain on nonuniform grids," *Radio Sci.,* vol. 31, pp. 905–912, July/Aug. 1996.
[15] J. S. Shang and R. M. Fithen, "A comparative study of characteristic-based algorithms for the Maxwell equations," *J. Comput. Phys.,* vol. 125, pp. 378–394, 1996.
[16] D. Kremer and R. Pregla, "The method of lines for the hybrid analysis of multilayered dielectric resonators," in *IEEE MTT-S 1995 Int. Microwave Symp. Dig.,* Orlando, FL, May 1995, pp. 491–494.
[17] D. Kajfez, A. W. Glisson, and J. James, "Computed modal field distributions for isolated dielectric resonators," *IEEE Trans. Microwave Theory Tech.,* vol. MTT-32, pp. 1609–1616, Dec. 1984.
[18] W. Zheng, "Computation of complex resonance frequencies of isolated composite objects," *IEEE Trans. Microwave Theory Tech.,* vol. 37, pp. 953–961, June 1989.

[19] J. A. Pereda, L. A. Vielva, A. Vegas, and A. Prieto, "Computation of resonant frequencies and quality factors of open dielectric resonators by a combination of the finite-difference time-domain (FDTD) and Prony's methods," *IEEE Microwave Guided Wave Lett.*, vol. 2, pp. 431–433, Nov. 1992.
[20] J. F. Lee and Z. Sacks, "Whitney elements time domain (WETD) methods," *IEEE Trans. Magn.*, vol. 31, pp. 1325–1329, May 1995.
[21] L. Zhao and A. C. Cangellaris, "A general approach for the development of unsplit-field time-domain implementations of perfectly matched layers for FDTD grid truncation," *IEEE Microwave Guided Wave Lett.*, vol. 6, pp. 209–211, May 1996.
[22] B. Chen, D. G. Fang, and B. H. Zhou, "Modified Berenger PML absorbing boundary condition for FD-TD meshes," *IEEE Microwave Guided Wave Lett.*, vol. 5, pp. 399–401, Nov. 1995.
[23] S. D. Gedney and U. Navsariwala, "An unconditionally stable finite element time-domain solution of the vector wave equation," *Microwave Guided Wave Lett.*, vol. 5, pp. 332–334, Oct. 1995.
[24] Y. B. Hua and T. K. Sarkar, "Generalized pencil-of-function method for extracting poles of an EM system from its transient response," *IEEE Trans. Antennas Propagat.*, vol. 37, pp. 229–234, Feb. 1989.
[25] R. K. Mongia, C. L. Larose, S. R. Mishra, and P. Bhartia, "Accurate measurement of Q-factors of isolated dielectric resonators," *IEEE Trans. Microwave Theory Tech.*, vol. 42, pp. 1463–1467, Aug. 1994.

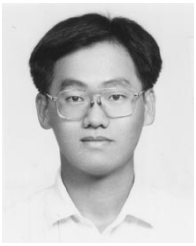

Chieh-Tsao Hwang was born in Tainan, Taiwan, R.O.C., in 1968. He received the B.S. (physics) and M.S. (electrical engineering) degrees from National Taiwan University, Taipei, Taiwan, R.O.C., in 1991 and 1993, respectively. He is currently working toward the Ph.D. degree at the same university.

His areas of interest include computational electromagnetics, dielectric resonator, transmission line discontinuities, and electromagnetic theory.

Ruey-Beei Wu was born in Tainan, Taiwan, R.O.C., in 1957. He received the B.S.E.E. and Ph.D. degrees from National Taiwan University, Taipei, Taiwan, in 1979 and 1985, respectively.

In 1982, he joined the faculty of the Department of Electrical Engineering and the Graduate Institute of Communication Engineering, National Taiwan University, where he is now a Professor. He was a Visiting Scholar at IBM, East Fishkill, NY, from March 1986 to February 1987 and in the Electrical Engineering Department, University of California, Los Angeles, from August 1994 to July 1995. Since 1998, he has been the Director of the National Center for High-Performance Computing, National Science Council, R.O.C. His areas of interest include computational electromagnetics, dielectric wavequides, edge-slot antennas, wave scattering of composite materials, transmission-line discontinuities, and interconnection modeling for computer packaging.